AFRL-ML-WP-TP-2006-413

AUTOMATIC GAP DETECTION IN FRICTION STIR WELDING PROCESSES (PREPRINT)

Yu Yang, Prabhanjana Kalya, Robert G. Landers, and K. Krishnamurthy

FEBRUARY 2006

MATERIALS AND MANUFACTURING DIRECTORATE
AIR FORCE RESEARCH LABORATORY
AIR FORCE MATERIEL COMMAND
WRIGHT-PATTERSON AIR FORCE BASE, OH 45433-7750

NOTICE AND SIGNATURE PAGE

AFRL-ML-WP-TP-2006-413 HAS BEEN REVIEWED AND IS APPROVED FOR PUBLICATION IN ACCORDANCE WITH ASSIGNED DISTRIBUTION STATEMENT.

//Signature//

DONNA L. BALLARD
Processing Section
Metals Branch

//Signature//

JEFFREY R. CALCATERRA, Section Chief
Processing Section
Metals Branch

//Signature//

GERALD J. PETRAK, Asst. Chief
Metals, Ceramics & NDE Division
Materials and Manufacturing Directorate

*Disseminated copies will show "//Signature//" stamped or typed above the signature blocks.

REPORT DOCUMENTATION PAGE	*Form Approved* *OMB No. 0704-0188*

1. REPORT DATE ***(DD-MM-YY)***	**2. REPORT TYPE**	**3. DATES COVERED** ***(From - To)***
February 2006	Conference Paper Preprint	07/01/2004 – 02/01/2006

4. TITLE AND SUBTITLE
AUTOMATIC GAP DETECTION IN FRICTION STIR WELDING PROCESSES (PREPRINT)

5a. CONTRACT NUMBER
FA8650-04-C-5704

5b. GRANT NUMBER

5c. PROGRAM ELEMENT NUMBER
78011F

6. AUTHOR(S)
Prabhanjana Kalya, Robert G. Landers, and K. Krishnamurthy (University of Missouri – Rolla)
Yu Yang (University of Southern California)

5d. PROJECT NUMBER
2865

5e. TASK NUMBER
25

5f. WORK UNIT NUMBER
25100000

7. PERFORMING ORGANIZATION NAME(S) AND ADDRESS(ES)
University of Missouri – Rolla
B. 37 McNutt Hall
1870 Miner Circle
Rolla, MO 65409-0340

University of Southern California
Department of Mechanical Engineering

8. PERFORMING ORGANIZATION REPORT NUMBER

9. SPONSORING/MONITORING AGENCY NAME(S) AND ADDRESS(ES)
Materials and Manufacturing Directorate
Air Force Research Laboratory
Air Force Materiel Command
Wright-Patterson AFB, OH 45433-7750

10. SPONSORING/MONITORING AGENCY ACRONYM(S)
AFRL-ML-WP

11. SPONSORING/MONITORING AGENCY REPORT NUMBER(S)
AFRL-ML-WP-TP-2006-413

12. DISTRIBUTION/AVAILABILITY STATEMENT
Approved for public release; distribution is unlimited.

13. SUPPLEMENTARY NOTES
This work, resulting in whole or in part from Department of the Air Force contract FA8650-04-C-5704, has been submitted to the Proceedings of 2006 ASME International Conference on Manufacturing Science and Engineering. If this work is published, ASME may assert copyright.

PAO Case Number: AFRL/WS 06-0661, 8 Mar 2006. This paper contains color content.

14. ABSTRACT
A common issue that arises when welding two plates is when a gap exists between the plates. This gap may be due to improper fixturing, imprecision in the processes used to manufacture the plates, etc. This paper develops a monitoring algorithm to detect gaps in Friction Stir Welding (FSW) processes. Experimental studies are conducted to determine how the process parameters and the gap width affect the welding process; particularly, the plunge force. The proposed monitoring algorithm examines the filtered plunge force in the frequency domain to determine the presence of gaps in FSW processes reliably.

15. SUBJECT TERMS
Friction Stir Welding, gap

16. SECURITY CLASSIFICATION OF:			**17. LIMITATION OF ABSTRACT:**	**18. NUMBER OF PAGES**	**19a. NAME OF RESPONSIBLE PERSON** (Monitor)
a. REPORT	**b. ABSTRACT**	**c. THIS PAGE**			Donna Ballard
Unclassified	Unclassified	Unclassified	SAR	26	**19b. TELEPHONE NUMBER** *(Include Area Code)* N/A

Standard Form 298 (Rev. 8-98)
Prescribed by ANSI Std. Z39-18

Automatic Gap Detection in Friction Stir Welding Processes

Yu Yang[1], Prabhanjana Kalya[2], Robert G. Landers[3], and Krishnamurthy[4]

Abstract

A common issue that arises when welding two plates is when a gap exists between the plates. This gap may be due to improper fixturing, imprecision in the processes used to manufacture the plates, etc. This paper develops a monitoring algorithm to detect gaps in Friction Stir Welding (FSW) processes. Experimental studies are conducted to determine how the process parameters and the gap width affect the welding process; particularly, the plunge force. The proposed monitoring algorithm examines the filtered plunge force in the frequency domain to determine the presence of a gap. Several experimental studies are conducted with a variety of process parameters and the monitoring algorithm is shown to be able to detect the presence of gaps in FSW processes reliably.

Introduction

Friction Stir Welding (FSW) is a new solid state welding technology [1,2,11,12] in which a rotating tool plunges into the intersection of two parts where material plastically deforms, due to an elevated temperature field, and the parts join as the tool leaves the processing zone. The FSW process has advantages in that it can weld materials that are difficult to weld using conventional

1 Department of Mechanical Engineering, University of Southern California, yuy@usc.edu
2 Department of Mechanical and Aerospace Engineering, University of Missouri at Rolla, pk34b@umr.edu
3 Department of Mechanical and Aerospace Engineering, University of Missouri at Rolla, landersr@umr.edu
4 Department of Mechanical and Aerospace Engineering, University of Missouri at Rolla, kkrishna@umr.edu

processes and is environmentally friendly since harmful gases are not required. A schematic of the FSW process for welding two plates (referred to in this paper as skin–to–skin welding) is shown in Figure 1. The tool consists of a pin and shoulder, both of which contact the part material, and slowly plunges into one plate where it dwells for a specified amount of time. Once the processing zone consists of plastically deformed material at an elevated temperature, the tool moves towards the other plate, typically at a specified velocity. When the tool travels from the first plate to the second plate a weld is formed between the two plates. While most welds are along the interface between the two plates, some welds are in the transverse direction and it is these type of welds that will be the focus of the studies in this paper.

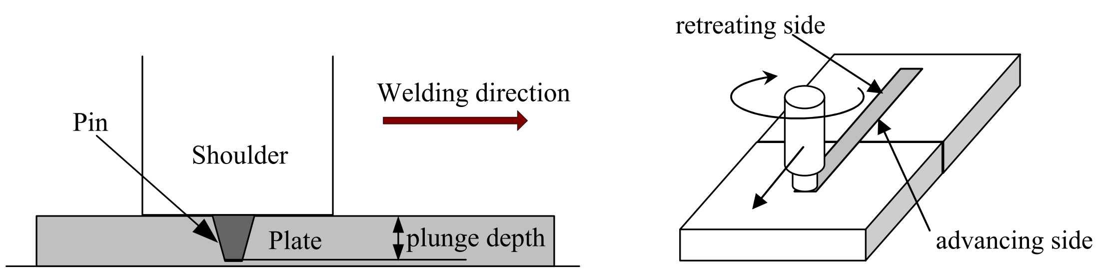

Figure 1: FSW Process Schematic.

Currently, research in FSW includes modeling the process with finite element method (FEM) [3] or numerical simulation [4], and examining process parameters effects [5,7]. In [6], a thermal model combined with a 2–D fluid mechanics based process model are utilized for simulation built. Models built with computational fluid dynamics (CFD) packages were introduced in [13,17]. In [16], an analytical model for heat generation in FSW processes is proposed. Material flow modeling [9] is another important area in research. In [8], material flow is analyzed with experimental methods and tool wear was taken into consideration in [10]. The effects of the FSW process on material properties is given in [14,15]. However, this modeling does not account for gaps that sometimes exist in the welding process and do not provide the knowledge one would need to construct a model–based monitoring algorithm.

A real–time monitoring algorithm that can robustly detect gaps in FSW processes is proposed in this paper. Given a model that relates the plunge force to the process parameters, a frequency analysis of the plunge force time history is utilized to detect the presence of a gap. The next section describes the experimental system utilized in this paper as well as initial experimental studies that shed light on the FSW process as gaps are encountered. The next section presents the monitoring algorithm and presents experimental results demonstrating that the monitoring technique can robustly detect the presence of gaps.

Experimental System and Initial Studies

The friction stir welding machine used for the experimental studies in this paper is shown in Figure 2. The machine has two axes, which are denoted *x* (perpendicular to the tool axis and in the direction of welding) and *z* (parallel to the tool axis and in the plunge direction), and a spindle with a maximum speed of 1550 *rpm*. The *x* and *z* axes are equipped with load cells capable of sensing forces up to 33.36 *kN* (7,500 *lbs*) and 88.97 *kN* (20,000 *lbs*), respectively. The control system is only capable of sensing forces with a 1 *Hz* sample frequency; therefore, the machine was augmented with a high speed data acquisition system (see Figure 3). The *x* and *z* axis and spindle encoders and *x* and *z* axis load cell signals were picked off and filtered through noise isolation circuitry. Note that the infrared temperature sensor is not used in the following experiments. The data is gathered by a National Instruments data acquisition system. The encoder signals are sensed via a counter timer board and the load cell signals are sensed via analog to digital channels on a multifunction board. A sample frequency of 100 *Hz* was utilized in all experimental studies. The axis and spindle velocities were calculated from the encoder data via first order backward difference schemes.

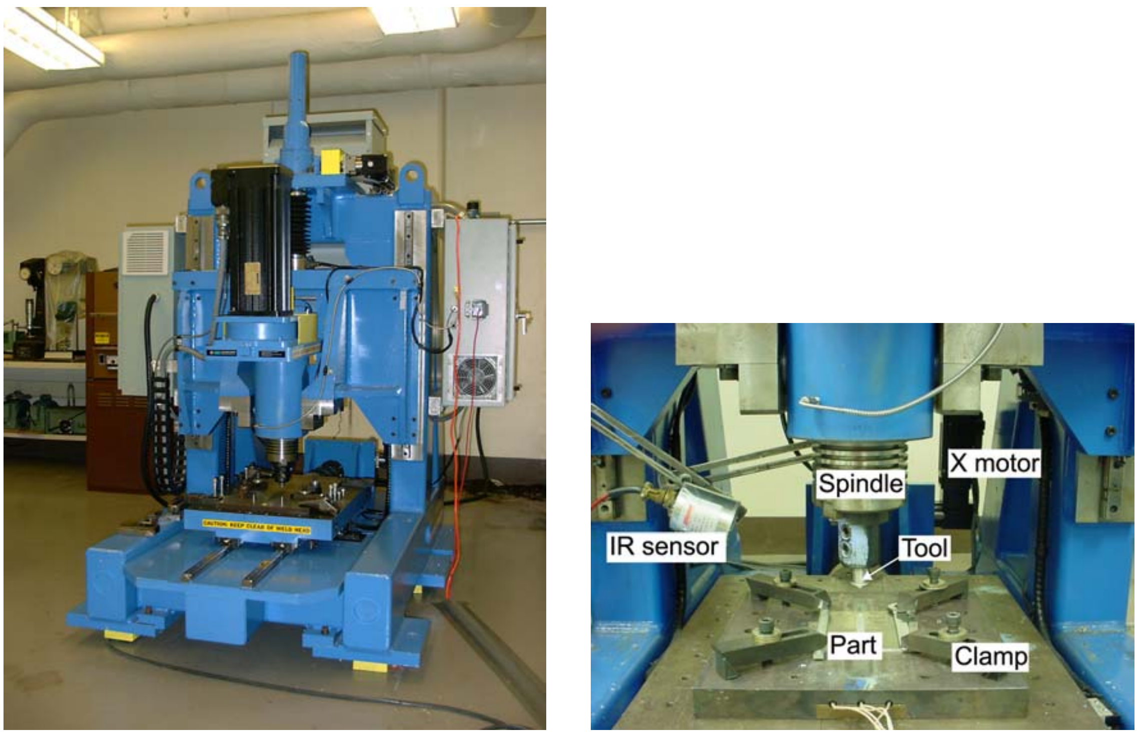

Figure 2: Friction Stir Welding Machine (left) and Experimental Setup (right).

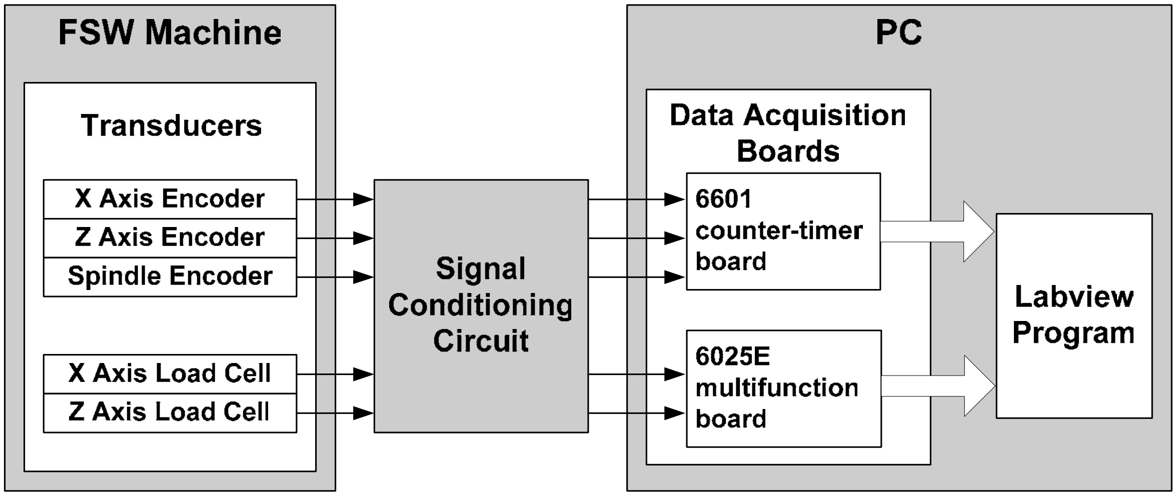

Figure 3: FSW Process Monitoring Data Acquisition System.

Initial experiments were conducted to derive a qualitative understanding of 2024 aluminum skin–to–skin FSW processes with and without gaps. Three different welding scenarios, as shown in Figure 4, were considered. The first scenario is referred to as "bead on plate." In this scenario the tool friction stirs a solid piece of material. The second scenario is referred to as "butt joint." In this scenario two plates are firmly pushed together such that there is no gap and then are welded. This scenario represents the ideal welding situation. The third scenario is referred to as "gap." In this scenario two plates are separated by shims such that there is a constant known gap and then are welded. This scenario represents the situation when the plates are separated due to improper fixturing, imprecise machining of the plates, etc. For all experiments conducted in this paper, the part material is a 2024 aluminum alloy with a T8 heat treatment, the tool is a proprietary tool from the Boeing company, the plate thickness is 3.175 *mm* (0.125 *in*), the plunge depth is 2.997 *mm* (0.1180 *in*), the plunge rotation speed is 1200 *rpm*, the plunge tool traverse rate is 0.0847 *mm/s* (0.2 *ipm*), the dwell time is 2 *sec*, and the tool tilt angle is 0^0. All data is sampled at a rate of 100 *Hz*.

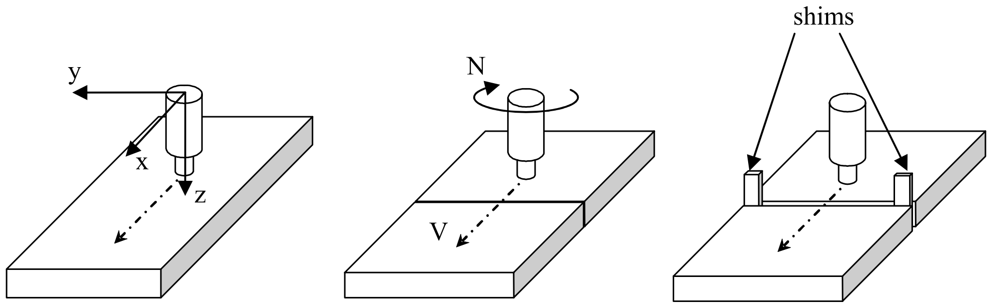

Figure 4: Skin–to–Skin Welding Scenarios: Bead on Plate (left), Butt Joint (middle), and Gap (right).

The plunge force time histories for the three skin–to–skin welding experiments with a rotation speed of 1000 *rpm*, a tool traverse rate of 4.233 *mm*/*s*, and a plunge depth of 2.997 *mm* are shown in Figure 5. The unfiltered force data is very noisy due to electrical noise in the circuits and noise due to the FSW process itself (e.g., random behavior in the material flow, nonlinear friction in the processing zone). Therefore, the raw force data was filtered with a three pole Butterworth digital filter with cutoff frequency of 4 *Hz*. The filter transfer function is

$$\frac{F_f(z)}{F(z)} = 10^{-3}\frac{0.2196z^3 + 0.6588z^2 + 0.6588z + 0.2196}{z^3 - 2.749z^2 + 2.528z - 0.7776} \quad (1)$$

where F_f is the filtered plunge force and F is the unfiltered plunge force. The filtering substantially removed the inherent noise, as shown in Figure 5. All of the experiments follow the same trend: the plunge force increases as the tool plunges into the material, the force decreases and then reaches a constant value as the tool dwells and the material temperature increases, and then the force increases as welding begins before reaching a higher steady state value. For the bead on plate experiment, the force remains constant until the tool retracts. For the butt joint experiment, there is a slight force variation, which cannot be seen on the graph, when the tool traverses the butt joint. This slight variation is due to the fact that the plate edges are not perfectly flat and slight gaps will exist between the plates even when great care is taken in the fixturing. For the gap experiment, there is a noticeable decrease in force when the tool traversed the 0.6858 *mm* (0.027 *in*) gap. The decrease in force is due to the fact that the tool encounters less material as it traverses the gap and material that is being processed while the tool traverses the gap can flow along the gap, thus, escaping the processing zone.

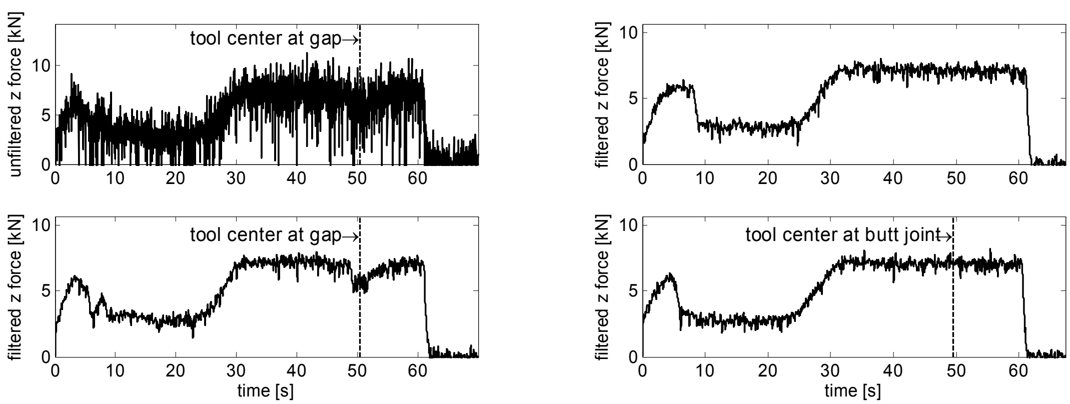

Figure 5: Plunge Force History for Various Experiments with *N* = 1000 *rpm* and *V* = 4.233 *mm/s* (10 *ipm*). Top left: 0.6858 *mm* (0.027 *in*) gap, forces unfiltered; bottom left: 0.6858 *mm* (0.027 *in*) gap, forces filtered; top right: bead on plate; bottom right: butt joint.

A series of bead on plate experiments were conducted to determine a model of the steady–state plunge force as a function of the process parameters (i.e., tool traverse rate and rotation speed). The experimental results are summarized in Table 1. The average plunge force is 7.0458 *kN* (1585 *lbs*) with a standard deviation of 0.0292 *kN* (6.564 *lbs*). Therefore, the process parameters do not significantly affect the steady–state plunge for the FSW operations considered in this study, they do not. While the process parameters do not affect the steady–state plunge force for the studies considered in this paper, the experiments demonstrate that the tool traverse rate affects the plunge force profile as the tool transverse the gap. As shown in Figure 6, the decrease in plunge force is inversely proportional to the tool traverse rate. This makes physical sense since the tool is in the gap region less when the tool traverse rate is higher.

Table 1: Bead on Plate Experiments for Model Development.

Experiment	Tool Traverse Rate, *mm*/*s* (*ipm*)	Rotation Speed, *rpm*	Steady–State Plunge Force, *kN* (*lbs*)
1	5.728 (13.53)	1141	7.050 (1585)
2	5.728 (13.53)	859	7.027 (1580)
3	4.233 (10)	1000	7.083 (1592)
4	4.233 (10)	1000	7.079 (1591)
5	2.735 (6.46)	1141	6.989 (1571)
6	2.735 (6.46)	859	6.981 (1569)
7	6.350 (15)	1000	7.045 (1584)
8	4.233 (10)	1200	7.054 (1586)
9	4.233 (10)	800	7.063 (1588)
10	2.117 (5)	1000	7.011 (1576)

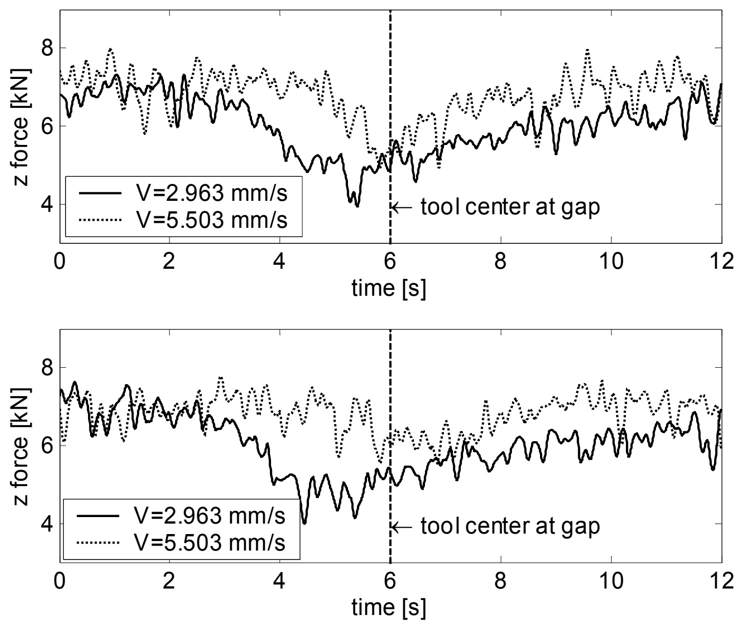

Figure 6: Plunge Force Time History during FSW Process with 0.6858 *mm* (0.027 *in*) Gap. Top Plot (*N* = 880 *rpm*) and Bottom Plot (*N* = 1120 *rpm*).

Gap Monitoring Algorithm and Experimental Results

A monitoring technique is developed in this section to automatically determine the presence of a gap. In the example shown in Figure 5, the gap width is 0.6858 *mm* (0.027 *in*) and the plunge force deviation as the tool transverses the gap is apparent. However, for smaller gap widths, the force deviation will be less, possibly within the range of the process noise. An example of this is shown in Figure 7. When the tool transverses a gap with a width of 0.3048 *mm* (0.012 *in*), the plunge force deviation is within same magnitude as the typical plunge force fluctuations. Therefore, it is difficult to judge whether or not a gap is present by using a plunge force, or a plunge force derivative, threshold value. However, the decreasing trend in the plunge force is still visible. To automatically detect this trend, frequency analysis is utilized.

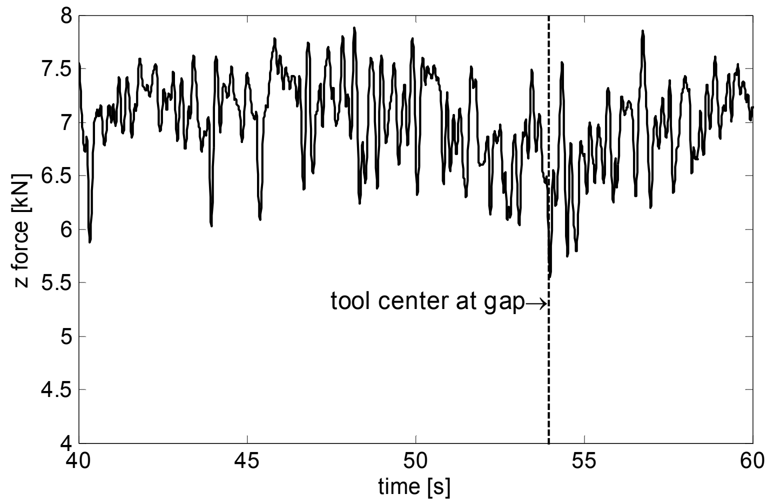

Figure 7: Plunge Force Time History: *N* = 1000 *rpm*, *V* = 4.233 *mm/s* (10 *ipm*), and a 0.3048 *mm* (0.012 *in*) Gap.

A Discrete Fourier Transform (DFT) is applied to the plunge force data to compute the signal power spectral density (PSD), which will be utilized to automatically monitor the presence of gaps. A complete DFT will provide a snapshot of the plunge force frequency content at a single moment in time. This computation is very time intensive and typically requires specialized computing hardware if it is to be performed in real–time. Therefore, the monitoring technique proposed in this paper will track the PSD at a specific frequency to determine the presence of gaps. The time history of the PSD at a specific frequency f (Hz) is defined as

$$P(t,f) = PSD\left(\Delta F\left(t-T,t\right):f\right) \quad (2)$$

where t is time (sec), T is data window size (sec), and the parameter F_a is

$$\Delta F\left(t\right) = F_f\left(t\right) - \text{mean}\left(F_f\left(t - T : t\right)\right) \tag{3}$$

where F_f is the filtered plunge force and $F_f(t–T,t)$ is the series of filtered plunge forces between time $t–T$ and t. The algorithm in equation (1) analyzes deviations in the plunge force from the nominal plunge force and tracks the power spectral density at a specific frequency using a moving set of data points. Experimental results for three different frequencies (0, 0.5 and 1 *Hz*) are shown in Figure 8. For these experiments, $T = 2$ *sec* (i.e., 200 samples are used for each PSD computation). Each frequency component sharply increases once the tool shoulder touched the gap and then decreased once the tool passed over the gap. Also, the magnitude of the increase is inversely proportional to the frequency, f.

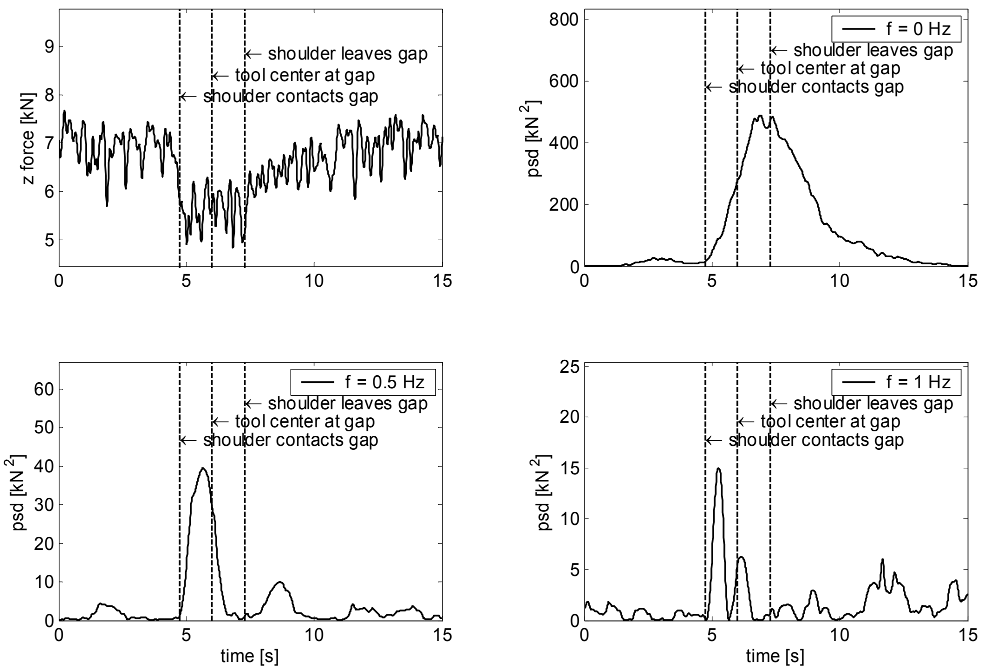

Figure 8: DFT Time Histories at Different Frequencies for FSW Experiments with *N* = 1000 *rpm*, *V* = 4.233 *mm*/*s* (10 *ipm*), and 0.6858 *mm* (0.027 *in*) gap. Top left: plunge force; top right: *f* = 0 *Hz*; bottom left: *f* = 0.5 *Hz*; bottom right: *f* = 1 *Hz*.

The largest change in the plunge force PSD occurs at a frequency of $f = 0$ Hz and, thus, this frequency is used for the gap monitoring algorithm developed in this paper. Using the zero frequency component also allows one to simplify the PSD computation, which becomes

$$P(t,0) = \frac{1}{N}\sum_{i=1}^{N} F_a^2(i) \tag{4}$$

where N is the number of data points used in the monitoring algorithm. This measurement, in effect, is a moving average that reflects the deviation of the plunge force from the steady–state plunge force.

The parameter *T* which, for a constant sample period, is proportional to the number of data samples, affects the gap monitoring algorithm. An example of this is shown in Figure 9. For 25, 50, 100, and 200 samples for each calculation, the gap monitoring algorithm recorded a PSD of 50 kN^2 at 4.6, 4.6, 4.2, and 4.1 *mm* before the gap, respectively. While the peaks are larger when more samples are utilized in the monitoring algorithm, the algorithm will sense the gap less quickly. Also, using more samples creates more computational burden. However, using too few samples will cause the algorithm to be unable to detect gaps. From the experimental results, *T* = 2 *sec* (i.e., 200 points) was selected.

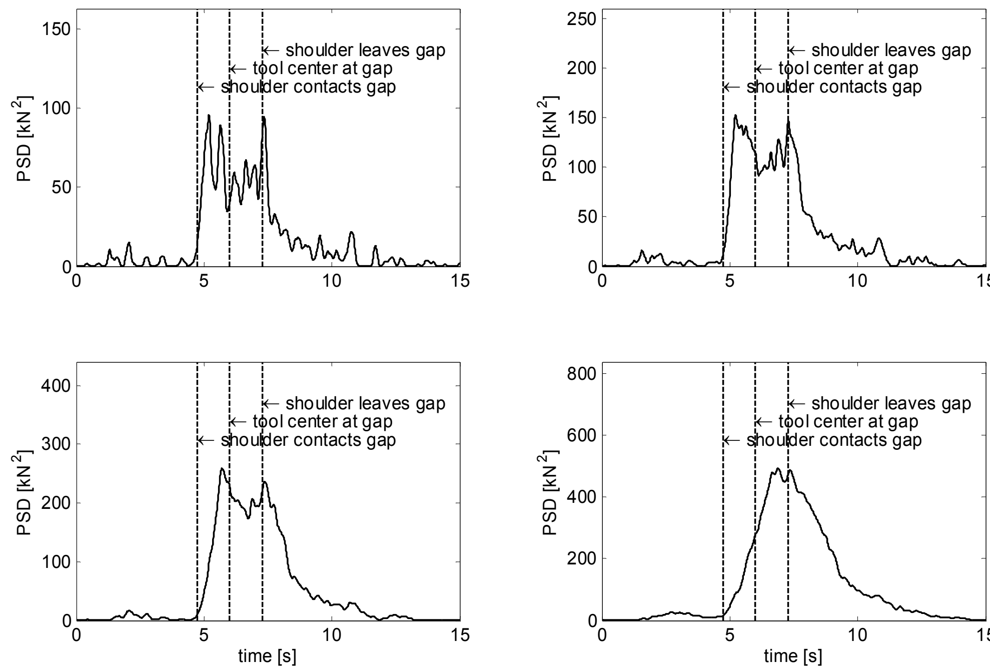

Figure 9: Experimental Results Demonstrating Effect of using Different Numbers of Samples in Gap Monitoring Algorithm with *N* = 1000 *rpm*, *V* = 4.233 *mm/s* (10 *ipm*), and 0.6858 *mm* (0.027 *in*) gap. Top left: 25 samples; top right 50 samples; bottom left 100 samples; bottom right 200 samples.

A set of experiments were conducted with various gap sizes, $N = 1000$ *rpm*, and $V = 4.233$ *mm/s* (10 *ipm*) and the results are shown in Figure 10. Like the plunge force, PSD magnitude increases with increasing gap width. For the butt joint, the PSD magnitude increased noticeably when the tool transversed the gap. This is due to the fact that the plates are not perfectly machined and, thus, are not completely flush against one another. While the increase is noticeable, it is highly dependent on the plate machining quality and is not significant enough to be reliably detected by an automatic algorithm. Based on the results in Figure 10, a threshold value of 50 kN^2 is determined to be sufficient to detect the presence of a gap. Like all thresholding techniques, the value determined here is only applicable to the particular process parameters and welding conditions considered in this study. For another FSW operation, further experimentation would be required to determine a suitable threshold value for the automatic monitoring algorithm.

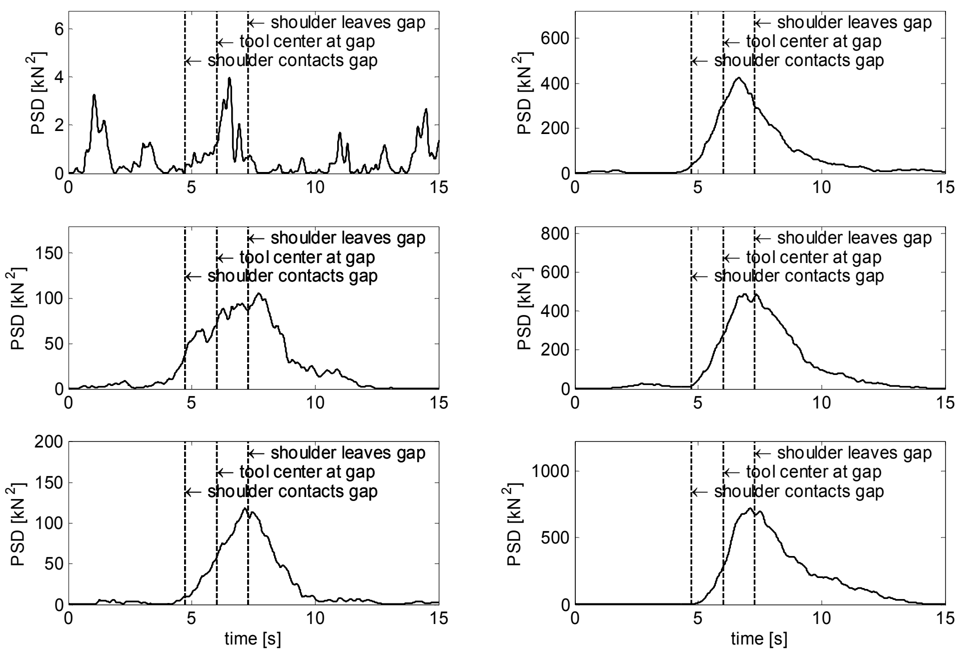

Figure 10: Experimental Results Demonstrating Effect of Gap with *N* = 1000 *rpm*, and *V* = 4.233 *mm/s* (10 *ipm*). Top left: butt joint; middle left: 0.3048 *mm* (0.012 *in*) gap; bottom left: 0.3810 *mm* (0.015 *in*) gap; top right: 0.5080 *mm* (0.020 *in*) gap; middle right: 0.6858 *mm* (0.027 *in*) gap; bottom right: 0.7874 *mm* (0.031 *in*) gap.

A set of experiments were conducted to validate the monitoring algorithm. The process parameters for each test are given in Table 2. In nine of the twelve cases, the gap was detected before the tool center was at the center of the gap and in seven of these cases, the gap was detected 2.5 *mm* or more before the tool center was at the gap center. In all cases the monitoring algorithm was able to detect the presence of a gap, even gaps as small as 0.3048 *mm* (0.0012 *in*) wide.

Table 2: Gap Detection Algorithm Experimental Results for Various Process Parameters.

Experiment	Tool Traverse Rate, *mm/s* (*ipm*)	Rotation Speed, *rpm*	Gap Width, *mm* (*in*)	Peak PSD Value, kN^2	Gap Detection Point, *mm*
1	2.963 (7)	880	0.3810 (0.0015)	202.18	3.85
2	2.963 (7)	880	0.6858 (0.0027)	840.91	6.16
3	5.503 (13)	880	0.3810 (0.0015)	207.40	–0.28
4	5.503 (13)	880	0.6858 (0.0027)	330.38	0.99
5	2.963 (7)	1120	0.3810 (0.0015)	485.92	4.62
6	2.963 (7)	1120	0.6858 (0.0027)	863.49	6.25
7	5.503 (13)	1120	0.6858 (0.0027)	119.47	–4.35
8	4.233 (10)	1000	0.3048 (0.0012)	63.77	–0.97
9	4.233 (10)	1000	0.7874 (0.0031)	688.53	2.92
10	2.117 (5)	1000	0.5080 (0.0020)	166.21	6.05
11	6.350 (15)	1000	0.5080 (0.0020)	91.08	0.32
12	4.233 (10)	1000	0.5080 (0.0020)	335.70	3.51

Summary and Conclusions

This paper presented a robust monitoring algorithm, which is applicable for real–time applications, for detecting gaps in friction stir welding (FSW) processes. A time history of the power spectral density of the delta plunge force is examined and a threshold value, which is determined experimentally, signals the presence of a gap. In this study, the delta plunge force is the average plunge force subtracted from the filtered plunge force. For other FSW operations, the plunge force will be a function of the process parameters. In this case, a model of the plunge force as a function of the process parameters can be constructed and the delta force will be the modeled force subtracted from the measured force. In this way, changes in process parameters will not affect the monitoring algorithm. The monitoring algorithm was applied to skin–to–skin FSW processes of a 2024 aluminum alloy. The results demonstrate the algorithm is able to reliably detect the presence of a gap for a wide range of processing parameters. Further, the gap was often detected well ahead of the pin entering the gap. This is due to the fact that the shoulder contacts the gap ahead of the pin. The algorithm developed in this paper will be useful in monitoring FSW processes and in performing intelligent control where process parameters are varied when defects such as gaps are encountered.

Acknowledgements

The authors wish to acknowledge the financial support for this work from the Air Force Research Laboratory (contract FA8650–04–C–5704) and the technical support of Rajiv Mishra from the University of Missouri at Rolla, David Bolser, Richard Lederich, and Raj Talwar from the Boeing company and Donna Ballard from the Air Force Research Laboratory.

References

1. Thomas, W.M., Nicholas, E.D., and Kallee, S.W., 2001, "Friction Based Technologies for Joining and Processing," *Friction Stir Welding and Processing*, Jata, K.V., Mahoney, M.W., Mishra, R.S., Semiatin, S.L., and Field, D.P., pp. 3–13.
2. Thomas, W.M., 2003, "Friction Stir Welding – Recent Developments," Materials Science Forum, *Thermec 2003 Processing and Manufacturing of Advanced Materials*, Madrid, Spain,

July 7–11, Vol. 426–432, No. 1, pp. 229–236.

3. Goetz, R.L., and Jata, K.V., 2001, "Modeling Friction Stir Welding of Titanium and Aluminum Alloys," *Friction Stir Welding and Processing*, Jata, K.V., Mahoney, M.W., Mishra, R.S., Semiatin, S.L., and Field, D.P., pp. 35–42.

4. Askari, A., Silling, S., London, B., and Mahoney, M., 2001, "Modeling and Analysis of Friction Stir Welding Process," *Friction Stir Welding and Processing*, Jata, K.V., Mahoney, M.W., Mishra, R.S., Semiatin, S.L., and Field, D.P., pp. 43–54.

5. Reynolds, A.P., and Tang, W., 2001, "Alloy, Tool Geometry, and Process Parameter Effects on Friction Stir Weld Energies and Resultant FSW Joint Properties," *Friction Stir Welding and Processing*, Jata, K.V., Mahoney, M.W., Mishra, R.S., Semiatin, S.L., and Field, D.P., pp. 15–23.

6. Reynolds, A.P., Khandkar, Z., Long, T., Tang, W., and Khan, J., 2003, "Utility of Relatively Simple Models for Understanding Process Parameter Effects on FSW," Materials Science Forum, *Thermec 2003 Processing and Manufacturing of Advanced Materials*, Madrid, Spain, July 07–11, Vol. 426–432, No.4, pp. 2959–2964.

7. Hattingh, D.G., Van, N., T.I., Blignault, C., Kruger, G., and James, M.N., 2004, "Analysis of the FSW Force Footprint and its Relationship With Process Parameters to Optimise Weld Performance and Tool Design," *Welding in the World*, Vol. 48, No. 1–2, pp. 50–58.

8. Blair, L., Murray, M., William, B., Michael, C., Richard, H.B., and Douglas, W., 2003, "Material Flow in Friction Stir Welding Monitored With Al–Sic and Al–W composite Markers," *Friction Stir Welding and Processing II*, Jata, K.V., Mahoney, M.W., Mishra, R.S., Semiatin, S.L., and Lienert, T., pp. 3–11.

9. Guerra, M., McClure, J.C., Murr, L.E., and Nunes, A.C., 2001, "Metal Flow During Friction Stir Welding," *Friction Stir Welding and Processing*, Jata, K.V., Mahoney, M.W., Mishra, R.S., Semiatin, S.L., and Field, D.P., pp. 25–34.

10. Prado, R.A., Murr, L.E., Rivera, A.R., Shindo, D.J., Soto, K.F., Fernandez, G.J., and McClure, J.C., 2003, "Tool Wear and Shape Optimization in the Friction Stir Welding of Aluminum Metal–Matrix Composites," *Friction Stir Welding and Processing II*, Jata, K.V., Mahoney, M.W., Mishra, R.S., Semiatin, S.L., and Lienert, T., pp. 23–32.

11. Chalmers, R.E., 2001, "The Friction Welding Advantage," *Manufacturing Engineering*, Vol. 126, No. 5, pp. 64–66,68,70.

12. Reitz, V., 2002, "Causing a Stir in Welding," *Machine Design*, Vol. 74, No. 6, pp. 59–61.

13. Reynolds, A.P., Lindner, K., Tang, W., and Seidel, T.U., 2002, "Weld Efficiency and Defect Formation: Correlation Between Experiment and Simple Models," *6^{th} International Trends in Welding Research Conference Proceedings*, Phoenix, Arizona, April 15–19, pp. 297–301.

14. Lockwood, W.D., Tomaz, B., and Reynolds, A.P., 2002, "Mechanical Response of Friction Stir Welded AA2024: Experiment and Modeling," *Materials Science and Engineering*, January 31, Vol. 323, pp. 348–353.

15. Chao, Y.J., Wang, Y., and Miller, K.W., 2001, "Effect of Friction Stir Welding on Dynamic Properties of AA2024–T3 and AA7075–T7351," *Welding Journal*, August, Vol. 80, pp. 196–200.

16. Schmidt, H., Hattel, J., and Wert, J., 2004, "An Analytical Model for the Heat Generation in Friction Stir Welding," *Modeling and Simulation in Materials Science and Engineering*, January, Vol. 12, No. 1, pp. 143–157.

17. Long, T., Seidel, T.U., Tang, W., and Reynolds, A.P., 2004, “A Friction Stir Welding Model Using Computational Fluid Dynamics,” *Hot Deformation of Aluminum Alloys III*, Jin, Z., Beaudoin, A., Bieler, T.A., and Radhakrishnan, B., pp. 299–312.